J. Membrane Biol. 94, 245–252 (1986)

The Journal of
Membrane Biology

Determination of Charge, Stoichiometry and Reaction Constants from *I-V* Curve Studies on a K^+ Transporter in *Nitella*

Joachim Fisahn, Ulf-Peter Hansen, and Dietrich Gradmann†
Institut für Angewandte Physik, Neue Universität, 2300 Kiel, Federal Republic of Germany and
†Pflanzenphysiologisches Institut, Untere Karspüle 2, 3400 Göttingen, Federal Republic of Germany

Summary. In *Nitella* cells with low pump activity, the electrical characteristics of membrane transport are mainly determined by K^+ transport. Current-voltage curves were measured at outside K^+ concentrations ranging from 0.1 to 100 mol m^{-3}. Above 1 mol m^{-3}, current saturated at positive and at very negative potentials. It was found that these *I-V* curves could be fitted by a Class I, case I reaction kinetic model, which is a cyclic reaction scheme with one pair of rate constants sensitive to membrane potential (Class I) and neutral transporter (or electrically charged substrate-transporter complex, case I). The analysis revealed the relative rate constants of a 3-state model. From the linear dependence of the rate constant of substrate binding (k_{32}) on $[K^+]_o$, the stoichiometry of 1 K^+/cycle was obtained. The complex transporter substrate is very unstable (very high value of k_{23}) resulting in a very low density of this state and in what can be called Mitchellian behavior; namely, the driving forces resulting from the electrical and from the concentration gradient can hardly be distinguished.

Key Words charge · Class I model · curve fitting · *I-V* curves · K^+ transporter · *Nitella* · reaction-kinetic model · rate constants · stoichiometry

Introduction

The measurement of current-voltage relationships of transporters in a biological membrane can lead to the estimation of reaction-kinetic data of the involved transport molecule, if the analysis is based on an appropriate reaction-kinetic model. Such a model is the Class I model (Hansen et al., 1981, 1984). The name Class I results from the restriction to cyclic reaction schemes with exactly one pair of rate constants being sensitive to membrane potential. This model was successfully applied to the analysis of electrogenic pumps (Mummert, Hansen & Gradmann, 1981; Gradmann, Hansen & Slayman, 1982; Beilby, 1984; Takeuchi et al., 1985) and to cotransporters (Sanders & Hansen, 1981; Sanders et al., 1984).

The simplicity of the analysis based on this model arises from the assumption of one central energy barrier which has to be overcome by the charged form of the transporter. The good fits obtained in the investigations mentioned above seem to verify this assumption in the cases of electrogenic pumps and of cotransporters. In the case of passive uniports, models with several binding sites in the "channel" were suggested (Kohler & Heckmann, 1979), which would render the *I-V* curve analysis very complicated.

However, patch-clamp data of a K^+ channel in *Vicia faba* (Schroeder, Hedrich & Fernandez, 1984) revealed the saturation phenomenon of the currents at very positive and at very negative potentials which are typical for models with recycling of the transport site. The analysis of these data and of some additional unpublished data provided by J.I. Schroeder showed that the Class I model could be applied to this K^+ channel and resulted in the identification of the charge of the transport site, and the numerical values of the involved rate constants (Gradmann, Klieber & Hansen, 1987[1]). These results encouraged us to apply the Class I analysis to the *I-V* curves of a K^+ channel in *Nitella*, especially as Lühring (1986) has found saturation at negative and at positive potentials in patch-clamp investigations of the *I-V* curves of a K^+ transporter in the cytoplasmic droplets of *Chara australis*. Beilby (1985) published an *I-V* curve obtained in *Chara* presoaked in 2 to 5 mol m^{-3} Na^+ which showed saturation at positive and negative potentials, but she thinks that these *I-V* curves are related to the proton pump.

Materials and Methods

Nitella flexilis was purchased from R. Kiel in Frankfurt and kept in APW (artificial pond water—0.1 mol m^{-3} KCl, 1.0 mol m^{-3} NaCl, 0.5 mol m^{-3} $CaCl_2$, no buffer) in the refrigerator at 10°C at a light intensity of 5 W m^{-2} (16 hr/day). pH was adjusted by small

[1] Gradmann, D., Klieber, H.G., Hansen, U.P. 1987. Reaction kinetic parameters for ion transport from steady-state current-voltage curves (*submitted*).

amounts of HCl, when the pH-meter showed deviations of 0.5 pH units. Short cells (2 cm length with a diameter of 0.5 mm) were selected in order to keep the cable problems small.

The cells in our laboratory showed the pecularity of low resting potentials of about −120 mV (so-called K^+ state; Beilby 1985, 1986*b*). This condition was very favorable for the investigations reported here, because (as the results presented here will show) the potassium transporter dominates the electrical characteristics of the membrane.

The experimental setup is described by Fisahn and Hansen (1986). Briefly, the APW described above flowed through a cooler and a heater which set the temperature to a desired value (15°C). Light intensity was zero. *I-V* curves (current-voltage relationships) were measured under voltage clamp. Two electrodes were inserted into the middle of the cell. In the tip of the preamplifiers there was a relay by which the electrode could be connected to the FET-OP 3140 (RCA) for the measurement of membrane potential, or via 10 kΩ to the output of the clamp-amplifier for current injection during the measurement of an *I-V* curve. It became necessary to change the solution in the current electrode from normally 10^3 mol m^{-3} KCl to 3×10^3 mol m^{-3} KCl plus 100 mol m^{-3} $AlCl_3$ in order to supply enough current to the cell. The clamp amplifier was homemade with a high-voltage OP (Burr Brown 3584 JM) supplying pulses up to ±110 V, and resulting in a settling time of the membrane potential of 2 msec.

For the measurement of the *I-V* curves under voltage clamp, a series of alternating impulses (120 + 80 + 120 + 80 msec for a subunit comprising resting potential, hyperpolarizing step, resting potential, depolarizing step) was used as described by Gradmann et al. (1978) in order to reduce the stimulating action on excitation processes and the development of negative resistance (Beilby, 1986*b*) which takes about 100 msec (Hansen, 1986). In our cells, at K^+ concentrations higher than 1 mol m^{-3}, there were no problems with long-lasting transients. An oscilloscope, permanently connected to the voltage- and to the current channel showed that current settled to a steady level within about 2 msec after the step in membrane potential. An Apple II microcomputer with a homemade interface board (comprising 12-bit A/D converters and 12-bit D/A converters, I/O ports for switching the relay and a real time clock for the protocol) measured the resting membrane potential for the calculation of the magnitude of the steps of the command voltage increasing from resting potential to the desired limits, switched the relay in the preamplifier selected for current injection 20 msec, and closed a second relay of the clamp loop 10 msec before the start of the pulse series. The computer stored the average of the current and of the potential (in order to check for insufficient clamp) during the last 10 msec of each of the steps mentioned above. The *I-V* curves could be displayed on the screen, or printed out or stored on diskette. For curve fitting the data were transferred to the PDP 10 of the Kieler Rechenzentrum via telephone modem. The program IV-MESS.PAS for Apple II or for IBM-compatible personal computers and the required interface boards are available on request.

For curve fitting of the *I-V* curves the programs PUMO.F10 or PUMA.ALG were used, which are improved versions of PUMO.FOR generated in 1979 in the laboratory of C.L. Slayman, New Haven, Connecticut.

Results

Measurement of the *I-V* Curves

I-V curves were measured at different concentrations of outside KCl ranging from 0.1 to 100 mol m^{-3}. The concentration of K^+ was changed without compensation by another ion, because the investigations on a K^+ channel in *Vicia faba* had shown that other ions such as Na^+ requires a class II model for the *I-V* curves of the transporter (Gradmann et al., 1987[2]). Control experiments in which chloride was replaced by sulfate did not reveal any significant differences.

Figure 1*A* displays such a set of *I-V* curves. The cells had problems to survive *I-V* curve measurements at high outside $[K^+]$. Thus, only a single full *I-V* curve was obtained from one cell at these concentrations. We took about 30 of these single *I-V* curves in the range of 20 to 100 mol m^{-3}, in order to make sure that they all showed the saturation phenomenon. The cells survived the measurement of a single curve, as tested by the repetition of the measurement of an *I-V* curve in low outside K^+ concentration. However, they scarcely could stand two subsequent runs at high outside K^+ concentrations.

This problem is the cause of the composition of the 100-mol m^{-3} curve in Fig. 1*A* from two experiments. The open squares of this curve belong to a data set comprising all concentrations, but with a restricted voltage range at high outside concentrations. Getting such a data set from one cell is necessary for the joint fit described below. In order to show that saturation really occurs, the 100-mol m^{-3} curve has been supplemented by data from an individual curve from a different cell (as mentioned above) scaled for coincidence in the common voltage range (filled squares).

In the range of positive potentials the density of data points is so high that the majority of them had to be omitted in order to give a clear picture. We decided to show those which do not coincide with the computer fit and to omit those which do.

A surprise was the finding that the cell could stand positive potentials up to +200 mV, and that there was little interference by action potentials and negative resistance (Beilby, 1986*b*). At the beginning we added 0.2 mol m^{-3} $LaCl_3$ to the bathing medium in order to prevent action potentials (Beilby, 1984), but later it was omitted because interference by action potentials was rare, even though the cells were excitable. Probably the suppression of action potential is a benefit of the alternative pulse series or of the low temperature (15°C). The resistivity of the cells to +200 mV may be related to the status of the cell. In our cells, pump activity was very low. However, it was not absent as temperature-induced changes of membrane potential (Fisahn & Hansen, 1986) and the 1-hr oscillation (Fisahn, Mikschl & Hansen, 1986) could be assigned to the modulation of the activity of a current source. Also, Keifer and Lucas (1982) assumed

[2] *See* footnote 1 on p. 245.

a low remaining pump activity in these cells. It may be that in the cells in the K^+ state (Beilby, 1986*a*) the membrane is tighter and can withstand higher positive potentials of short duration (40 msec) than other cells. Recently, Beilby (1986*b*) measured *I-V* curves in *Chara* up to +200 mV. Whatever the reason for this insensitivity, it was of great value for the investigations reported here, because it opened the access to the positive saturation region.

A visual inspection of the *I-V* curves in Fig. 1*A* shows that there is little effect of the K^+ concentration on the saturation currents measured at positive membrane potentials and that the steepness of the curves increases with increasing K^+ concentration. A more powerful discussion of these effects is enabled by curve fitting of the data.

Curve Fitting

The genuine model for the description of an individual Class I I-V curve is the 2-state model (Hansen et al., 1981), because the number of free parameters fits exactly the information enclosed in a single *I-V* curve. In this 2-state model, the involved rate constants are merged into four "apparent" reaction constants by means of so-called reserve factors accounting for the hidden states of the transport molecule. These four reaction constants are k_{io} and k_{oi} for the electro-sensitive reactions and κ_{io} and κ_{oi} for the neutral recycling reactions, which determine the positive and the negative saturation currents, respectively, in the case of a positively charged transporter-substrate complex. Consequently, the experimental access to individual rate constants of an *n*-state model is impossible if single *I-V* curves are investigated.

The experimenter gets closer to the "real" rate constants, if sets of *I-V* curves obtained at different experimental conditions are analyzed, because the additional information supports the construction of models with more than 2 states. Gradmann et al. (1987)[3] have shown that the investigation of the influence of substrate concentration enables the construction of a 3-state model. In this 3-state model, all rate constants can be determined if the translocated complex substrate transporter is electrically charged. One rate constant remains unknown if the complex is neutral.

There are two ways to calculate the 3-state model from the measured *I-V* curves. One way is to fit the individual *I-V* curves by 2-state models, and then calculate the 3-state rate constants from two sets of 2-state parameters obtained at different concentrations of the substrate. This method is very sensitive to numerical problems, because differences of nearly equal numbers occur in the denominators of the related equations (Gradmann et al., 1987[4]). The second way is a joint fit of the whole set of *I-V* curves using an appropriate 3-state model. As this way suffers less from numerical problems, it is used for the analysis here.

At first, the correct 3-state model has to be selected. The insets of Fig. 1*A* and Fig. 1*B* show the two alternatives. In Fig. 1*A* the complex substrate transporter carries electrical charge. In Fig. 1*B* it is the unloaded transporter. The two models can be distinguished by the dependence of the 2-state parameters on substrate concentration (Gradmann et al., 1987[5]). The first criterion is the dependence of the saturation currents on substrate concentration. The inspection of Fig. 1*A* shows that the negative saturation current (κ_{io} in case I and κ_{oi} in case II) increases with the substrate concentration, as predicted for either model. However, the positive saturation current stays constant. This is postulated by case II, but it does not exclude case I, as the changes of substrate may not have reached the range where the dependence becomes obvious (*see* discussion of Fig. 4).

The second criterion deals with the steepness of the curves. In case I, it increases with substrate concentration, whereas it decreases in case II. Fig. 1*A* shows that case I applies.

For case I, the following equation has to be used:

$$i = \frac{zFN_o(k_{12}k_{23}k_{31} - k_{21}k_{32}k_{13})}{k_{12}(k_{23} + k_{32} + k_{31}) + k_{21}(k_{13} + k_{32} + k_{31}) + k_{13}(k_{23} + k_{32}) + k_{31}k_{23}} \quad (1)$$

with

$$k_{12} = k_{120} \exp(zFV/2RT)$$
$$\text{and } k_{21} = k_{210} \exp(-zFV/2RT) \quad (2a,b)$$

introducing the dependence on membrane potential V. The names of the reaction constants refer to the numbers of the states shown in the insets of Fig. 1*A* and Fig. 1*B*. The model in Fig. 1*A* postulates that the rate constant of the binding of the substrate, k_{32}, should change with the outside concentration of the substrate

$$k_{32} = k_{320}S^n \quad (3)$$

with

$$S = [K^+]_o \quad (4)$$

[3] *See* footnote 1 on p. 245.

[4] *See* footnote 1 on p. 245.

[5] *See* footnote 1 on p. 245.

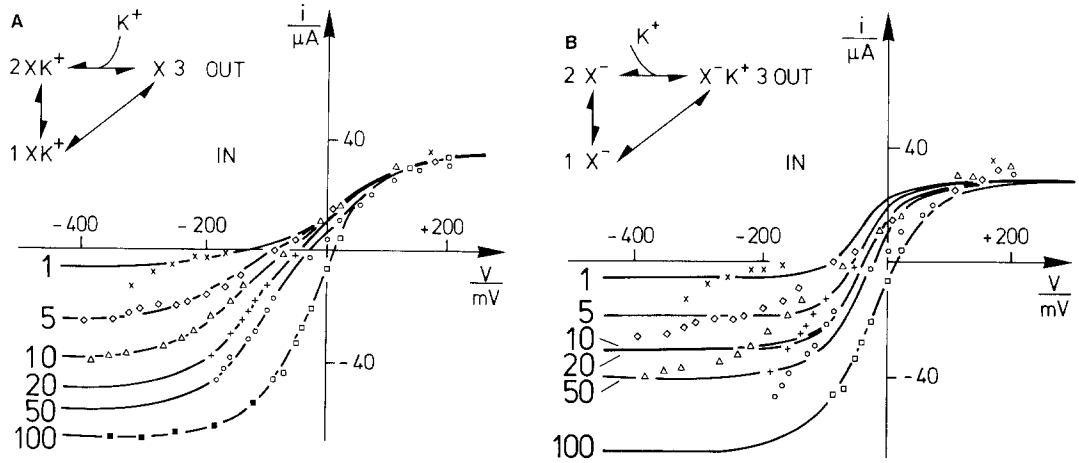

Fig. 1. Set of current voltage curves obtained from *Nitella* at different concentrations of outside K^+ subject to curve fitting on the basis of Eqs. (1) and (2). For reasons described in the text, the 100-mol m^{-3} curve in Fig. 1*A* is composed of data from two different cells. The numbers attached to the curves give the concentration of $[K^+]_o$ in mol m^{-3}. At positive potentials not all data points are shown, because they coincide and hide each other. The currents are input currents of the whole cell, length 2 cm, diameter 0.5 mm. $T = 15°C$. The numbers in the reaction schemes in the insets are the state numbers used in the names of the reaction constants. (*A*) Curve fitting by case I (neutral carrier as shown in the inset). Joint fit with all reactions constants but k_{32} kept equal for all sets. Numerical data: $k_{12^0} = 50.6$, $k_{21^0} = 1102$, $k_{23} = 45{,}800$, $k_{32^0} = 12.8$, $k_{31} = 34.3$, $k_{13} = 70.7$. These data include zFN_o, dimension μA, besides k_{32^0}: $\mu A/(\text{mol } m^{-3})$. (*B*) "The wrong model." Curve fitting of the same data set by case II, i.e., joint fit with k_{23} being free instead of k_{32}

and that all other rate constants have to be the same for the whole set of curves in Fig. 1. n is the stoichiometry of substrate binding.

In order to test the hypothesis that the Class I-case I model applies, the data were subject to a joint fit in which the computer had to use common values for five of the reactions constants in all data sets, and was allowed to choose different values for k_{32}. The data were also fitted on the basis of case II. In Fig. 1*B*, a case II fit of the data of Fig. 1*A* is shown. The comparison of Fig. 1*A* and Fig. 1*B* makes obvious that case II can be definitely ruled out. The case II model (charged transport site) cannot increase the steepness of the *I-V* curve with substrate concentration (Gradmann et al., 1986[6]). As seen from Fig. 1*B* this feature results in the failure of the fits: the case II model cannot adjust the slope to the data in the voltage-sensitive region. The attempts of the curve-fitting routine to minimize the errors in the slope region transfer the error also to the saturation regions.

In the fits based on case I (neutral transport site) shown in Fig. 1*A*, good fits are obtained at substrate concentrations higher than 1 mol m^{-3}, whereas at lower concentrations the current increases over the saturation currents suggested by the computer, especially at negative potentials as shown by the downward bending off from the computer fit. Obviously, these curves cannot be fitted by a single Class I model, because the current increases to values higher than the saturation current at low substrate concentration.

There are two possible explanations. Firstly, the low K^+ concentrations exert secondary effects on the transporter, changing its kinetic constants in a complicated way. However, we favor the second explanation, that at low $[K^+]_o$ a second transporter is involved. Beilby (1985, 1986*a*) and Sokolik and Yurin (1981, 1986) propose that a so-called leak determines the electrical behavior at $[K^+]_o$ below 1 mol m^{-3}. On the other hand, Coster and Hope (1968) and Tyerman, Findlay and Paterson (1986*a*,*b*) reported an increase of chloride fluxes at negative potentials.

The fits of the curves for $[K^+]_o$ higher than 1 mol m^{-3} gave very good fits. The averages obtained from four sets are shown in the Table. In order to illustrate the information obtained from the analysis, the rate constants of the Table are attached to the Class I, case I model in Fig. 2. These reaction constants include the unknown number of transporters N_o and the factor zF in Eq. (1). The determination of the reaction constants themselves would require the determination of N_o, which could be done by patch-clamp experiments (Gradmann et al., 1986[7]), or by the measurement of the temporal behavior (Tittor et

[6] *See* footnote 1 on p. 245.

[7] *See* footnote 1 on p. 245.

Table. The 3-state reaction constants (dimension is sec $^{-1}$ for $zFN_o = 1$, except for k_{320} which is sec $^{-1}$ mol $^{-1}$ m^3) obtained from curve fitting of four data sets by Eq. (1)[a]

	k_{120}	k_{210}	k_{23}	k_{320}	k_{31}	k_{13}
Value	40.6	373.3	37372	19.4	35.1	55.7
Scatter	1.2	2.7	3.7	1.5	1.1	1.2

[a] The scatter is given as a factor according to averaging in a logarithmic scale.

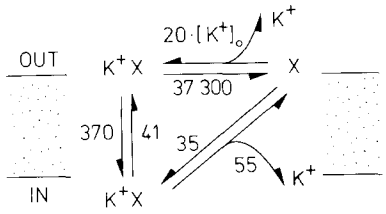

Fig. 2. The 3-state model (case I) selected for the analysis with the numerical values of the Table obtained from averaging the fits of the curves similar to those in Fig. 1 attached to the rate constants. The value of k_{32} is that for 1 mol m^{-3}. Its dependence on $[K^+]_o$ is given in Fig. 3. The values include the unknown number of transporters N_o and zF

al., 1983). The analysis of the temporal behavior requires a model, which has not yet been developed for this transporter.

In Fig. 3, the dependence of k_{32} on $[K^+]_o$ is plotted. In order to show the high reproducibility of the results, three individual experiments are displayed. Figure 3 shows that the reaction constant k_{32} is independent of $[K^+]_o$ for concentrations below 1 mol m^{-3}. It increases linearly with the slope 1 at concentrations between 2 and 100 mol m^{-3}. From this slope, the stoichiometry of substrate binding in Eq. (3) is determined. It is 1 K^+/transport cycle.

As mentioned above, the 2-state model is the adequate tool of describing the curve-shape of *I-V* curves. Thus, the 2-state parameters have been calculated from the 3-state fits by means of the following set of equations:

$$k_{io} = k_{12}/r_1 = k_{12}(k_{31} + k_{32})/(k_{31} + k_{32} + k_{13}) \quad (5a)$$

$$k_{oi} = k_{21}/r_2 = k_{21}(k_{31} + k_{32})/(k_{31} + k_{32} + k_{23}) \quad (5b)$$

$$\varkappa_{io} = \varkappa_{132}/r_1 = k_{13}k_{32}/(k_{31} + k_{32} + k_{13}) \quad (5c)$$

$$\varkappa_{oi} = \varkappa_{231}/r_2 = k_{23}k_{31}/(k_{31} + k_{32} + k_{23}) \quad (5d)$$

with the reserve factors

$$r_1 = (k_{31} + k_{32} + k_{13})/(k_{31} + k_{32}) \quad (6a)$$

$$r_2 = (k_{31} + k_{32} + k_{23})/(k_{31} + k_{32}). \quad (6b)$$

The reserve factors are a measure of the amount of the states of the 3-state model represented by the states of the 2-state model (Hansen et al., 1981, redefined by Hansen et al., 1983):

$$N_{1,2\text{-state}} = r_1 N_{1,3\text{-state}} \quad (7a)$$

$$N_{2,2\text{-state}} = r_2 N_{2,3\text{-state}}. \quad (7b)$$

The dependence of the 2-state parameters calculated from the data in Fig. 1 by means of Eqs. (5a) to (5d) are displayed in Fig. 4, and, of course, reflect the features seen in Fig. 1*A*.

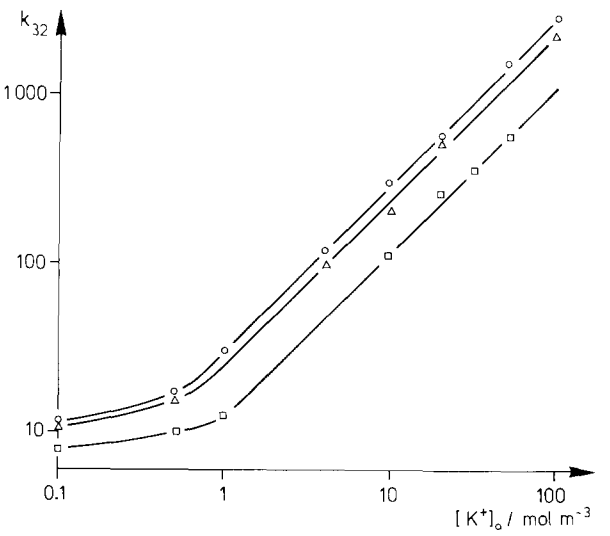

Fig. 3. Dependence of k_{32} on $[K^+]_o$ shown for three individual experiments. The smooth lines are eye fits

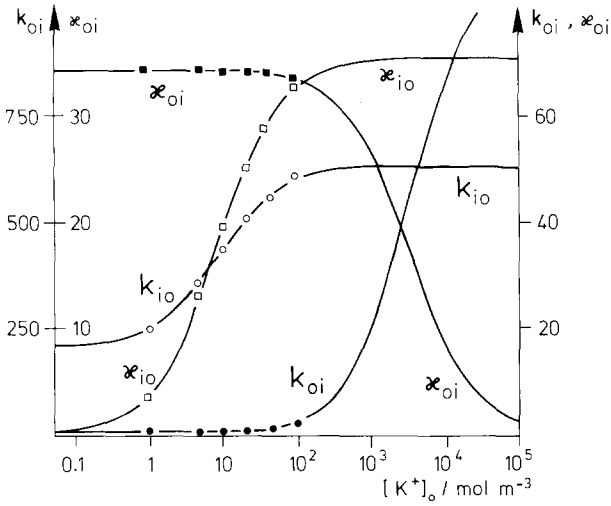

Fig. 4. The dependence of the 2-state parameters on substrate concentration $[K^+]_o$ as calculated from the reaction constants by means of Eqs. (5a) to (5d) and Eq. (3) obtained from the fit shown in Fig. 1*A*. The data points are the 2-state parameters calculated from the fits of the *I-V* curves in Fig. 1*A* at different $[K^+]_o$

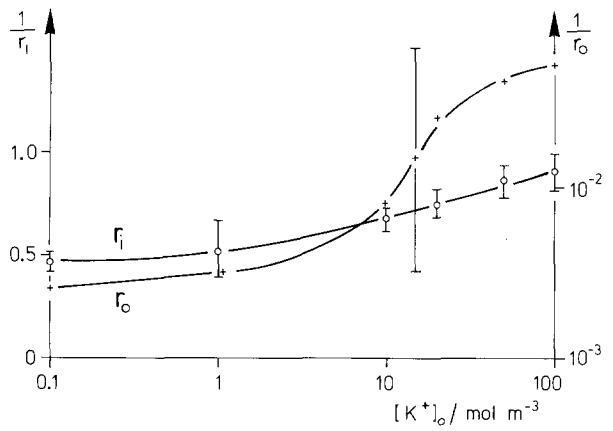

Fig. 5. The dependence of the inverse reserve factors $1/r_i$ and $1/r_o$ (Eqs. 6 to 8) on $[K^+]_o$. They are a measure of the probability of finding the transporters in state 2 or state 1, respectively, obtained from averaging for data sets. In the case of $1/r_i$ the scatter is shown at the individual data points. Because of the enormous magnitude of the scatter of $1/r_o$ (which results from the high value of k_{23}), the average scatter factor of 4.5 is shown only once. $r_i = r_1$, $r_o = 2$

However, the insertion of the reaction constants obtained from curve-fitting into Eq. (1) enables also the extrapolation of the data, in order to see what phenomena would be observed at concentrations outside the applied range of $[K^+]_o$ from 0.1 to 100 mol m^{-3}. The positive saturation current κ_{oi} stays nearly constant over the whole range of investigated concentrations. The mathematical extrapolation of the data on the basis of Eq. (5c) and Eq. (3) shows that a decrease occurs at concentrations higher than 100 mol m^{-3}. *Nitella* as well as KCl dislike these high concentrations up to 10^5 mol m^{-3}. Thus, the changes in the positive saturation current cannot be observed. This is the reason that the dependence of κ_{oi} on $[K^+]_o$ fails as a means of distinguishing between case I and case II as mentioned above.

In the investigated range of concentrations, the increase of k_{io} and κ_{io} is similar. Thus, there is an effect on the steepness as well as on the negative saturation current. This feature explains that the negative saturation current does not increase proportional to outside substrate concentration, but only by a factor of 10 when substrate increases by a factor of 100.

The inverse reserve-factors $1/r_1$ and $1/r_2$ are shown in Fig. 5. They are a measure of the distribution of transporters between state 1 and state 3 or between state 2 and state 3 in the 3-state model, because of the relations

$$N_1 = N_3/(r_1 - 1) \quad (8a)$$

$$N_2 = N_3/(r_2 - 1). \quad (8b)$$

$1/r_1$ changes from 0.5 to 0.8 over the whole range of $[K^+]_o$ indicating that the densities of state 1 and of state 3 in the 3-state model are about equal. However, $1/r_2$ takes very small values, showing that the density of transporters in state 2 is very low.

Discussion

The analysis above has shown that the *I-V* curves of the investigated K^+ transporter in *Nitella* can be described by the Class I model originally developed for electrogenic pumps. From this investigation, the following knowledge is obtained:

1. The investigated K^+ transporter in *Nitella* can be described by a Class I model. This finding has two implications:

   a. It may be regarded as less surprising that the transporter is not yet a water-filled hole, but a more complicated structure in which the binding site has to be recycled. The back reactions of the binding site after the discharge of the substrate are the cause of the saturation regions as given by the rate constants κ_{io} and κ_{oi}. These back reactions should not be visualized as translocations of a carrier like valinomycin, but may be a change of the accessibility of the binding site from one side to the other.

   b. The successful fit on the basis of Eq. (1) and Eqs. (2a,b) indicates that the assumption of one dominating energy barrier in the "channel" is legitimate. This consequence of our results may be considered to be more surprising than the obvious rejection of the water-filled hole, because in the case of "channels" complicated energy profiles were considered (Kohler & Heckmann, 1979). The fits in Fig. 1*A* show that there are channels with a lower degree of sophistication than anticipated.

2. The increase of the steepness with substrate concentration assigns case I to the transporter, i.e., the recycling of the binding site is electroneutral, and the complex transporter substrate carries positive charge. Additional support for the validity of case I is provided by the complete failure of case II to fit the slopes of the data as shown in Fig. 1*B*.

3. The curve-fitting routine allows the determination of the reaction constants of the Class I, case I 3-state model (Fig. 2). As mentioned above, the reaction constants in the Table comprise the factors z (=1), F and N_o, the number of involved transporters. Whereas F is known, N_o, can be determined only by patch-clamp experiments (Gradmann

et al., 1987[8]) or by nonsteady-state investigations (Tittor et al., 1983). These experiments are not available at the moment, and thus the data in the Table have to be considered as relative reaction constants.

4. The scatter shown in the second line in the Table tells about the accuracy with which the individual reaction constants can be determined by experiments of this kind. This accuracy depends on the degree by which the reaction constants influence the measured *I-V* curves. The best accuracy is obtained for k_{31} and k_{13} (scatter factor 1.2 and 1.1, respectively), because they are closely related to the saturation currents $zF\kappa_{io}N_o$ and $zF\kappa_{oi}N_o$, which can be measured with good accuracy. k_{23} and k_{32} are in series with k_{31} and k_{13}, but have higher numerical values. Thus, their influences on the saturation currents are much smaller (*see* Eqs. 4a to 4d), and their determination is more difficult as seen from the scatter factors of 3.7 and 1.5. In the case of k_{23}, the scatter factor of 3.7 (i.e., a quarter of 37,00 and the fourfold value are within the variance) implies that the information obtained from these experiments is restricted to the statement "k_{23} is much larger than the other reaction constants." The reserve factor r_o (Fig. 5) transfers the high scatter of k_{23} to the high scatter (factor 2.7) of k_{21}. The low scatter of k_{12} results from the significant changes in steepness with $[K^+]_o$, which were mentioned above as a means of distinguishing between case I and case II.

5. The numerical values of the rate constants in Fig. 3 and in the Table reveal some pecularities of the transporter which are discussed now. The dominant feature is the high backward reaction k_{23}. The asymmetry of k_{23} and k_{32} has several consequences:

a. The state 2 (Fig. 3) is very unstable, and thus a very small amount of the transporters is in this state.

b. N_2 is a reference state of the 2-state model. As the density of state 3 is much higher than that of state 2, the reserve factor r_o becomes very large (Fig. 5).

c. The reserve factor r_o depends strongly on substrate concentration which influences the ratio of k_{23} to k_{32}. This strong dependence of r_o on substrate concentration results in the so-called "sensitivity transfer" (Hansen et al., 1981). Sensitivity transfer implies that the naive expectation that outside substrate concentration would exclusively influence κ_{io}, and thus would increase the negative saturation current linearly, does not hold. Instead, an increase of the electro-sensitive translocation is found which results in an increased relative steepness.

This transfer of the substrate effect from the neutral limb to the k rate constants is called Mitchellian behavior, because the driving forces resulting from the electrical and from the concentration gradient are merged (Mitchell, 1966; Hansen et al., 1981).

6. The most convincing evidence for the validity of the model in Fig. 2 is the linear dependence of k_{32} shown in Fig. 3. This linearity assigns the stoichiometry of 1 to the binding of K^+. Recently, Smith (1986) and Smith, Smith and Walker (1986) have reanalyzed the old problem that the conductances calculated from K^+ fluxes do not match those calculated from electrical measurements. By means of an improved experimental approach (simultaneous measurement) they found that at K^+ concentrations above 1 mol m^{-3} this discrepancy does not exist. Their interpretation in terms of the Goldman hypothesis has one result in common with this investigation: the involved transporter has a single binding site.

7. The linear relationship shown in Fig. 3 ends at concentrations below 1 mol m^{-3}. This finding resembles the behavior of the reversal potential of passive transport in *Nitella* (Fisahn & Hansen, 1986; Fisahn et al., 1986) and in *Eremosphaera* (Köhler et al., 1985): Below 1 mol m^{-3} $[K^+]_o$, the reversal potential stays constant at −120 mV. There are two possible explanations:

a. K^+ is accumulated in the cell wall, and thus the plasma membrane does not sense a decrease of $[K^+]$ in the bathing medium.

b. At low $[K^+]_o$, a different transporter dominates membrane potential. This transporter is favored by Beilby (1985, 1986*a*). She regarded it as an unspecific leak, but now she has found K^+ sensitivity (1986*b*) similar to Sokolik and Yurin (1981, 1986).

The first alternative seems unlikely as Abe and Takeda (1986) have found the saturation of membrane potential also in isolated protoplasts of *Nitella*. We think it is unlikely, that the unstirred layer of the protoplast has the same effect as the cell wall of the intact cell, even though it cannot be excluded. However, in many experiments, we found a different type of *I-V* curves at $[K^+]_o = 0.1$ mol m^{-3}, namely, *I-V* curves bending up at positive and down at negative potentials as seen for the 0.1-curve at negative potentials in Fig. 1*A*.

[8] *See* footnote 1 on p. 245.

We are grateful to the Deutsche Forschungsgemeinschaft for financial support (Ha 712/7-3). Thanks are due to Dr. M.J. Beilby for helpful discussions, to E. Mikschl, J. Kolbowski and R. Willkomm for their assistance during the construction of the data-acquisition system, to H. Mainzer for the building of the clamp amplifier, and to Mrs. E. Götting for drawing the figures.

References

Abe, S., Takeda, J. 1986. The membrane potential of enzymatically isolated *Nitella expansa* protoplasts as compared with their intact cells. *J. Exp. Bot.* **37:**238–252

Beilby, M.J. 1984. Current-voltage characteristics of the proton pump at *Chara* plasmalemma: I. pH dependence. *J. Membrane Biol.* **81:**113–125

Beilby, M.J. 1985. Potassium channels at *Chara* plasmalemma. *J. Exp. Bot.* **36:**228–239

Beilby, M.J. 1986*a*. Potassium channels and different states of *Chara* plasmalemma. *J. Membrane Biol.* **89:**241–249

Beilby, M.J. 1986*b*. Factors controlling the K^+-conductance in *Chara*. *J. Membrane Biol.* **93:**187–193

Coster, H.G.L., Hope, A.B. 1968. Ionic relations in cells of *Chara australis*. XI. Chloride fluxes. *Aust. J. Biol. Sci.* **21:**243–254

Fisahn, J., Hansen, U.P. 1986. The influence of temperature on a K^+-channel and on a current-source in *Nitella*. *J. Exp. Bot.* **37:**440–460

Fisahn, J., Mikschl, E., Hansen, U.P. 1986. Separate oscillations of a K^+-channel and of a current-source in *Nitella*. *J. Exp. Bot.* **37:**34–47

Gradmann, D., Hansen, U.P., Long, W.S., Slayman, C.L., Warncke, J. 1978. Current-voltage relationships for the plasma membrane and its principal electrogenic pump in *Neurospora crassa*: I. Steady-state conditions. *J. Membrane Biol.* **39:**333–367

Gradmann, D., Hansen, U.P., Slayman, C.L. 1982. Reaction kinetic analysis of current-voltage relationships for electrogenic pumps in *Neurospora* and *Acetabularia*. *Curr. Top. Membr. Transp.* **16:**257–276

Hansen, U.P. 1986. Reaction kinetic models of pumps, cotransporters and channels. *In:* Ion Channels and Electrogenic Pumps in Biomembranes. Abstracts of Lectures and Posters. pp. L13–L33. Osaka University, Japan

Hansen, U.P., Gradmann, D., Sanders, D., Slayman, C.L. 1981. Interpretation of current-voltage relationships for "active" ion transport systems: I. Steady-state reaction-kinetic analysis of class-I mechanisms. *J. Membrane Biol.* **63:**165–190

Hansen, U.P., Gradmann, D., Sanders, D., Tittor, J., Slayman, C.L. 1984. Steady-state and non-steady state models of membrane transport. *In:* Membrane Transport in Plants. J. Cram, K. Janacek, R. Rybova, and K. Sigler, editors. pp. 33–38. Akademia, Prague

Keifer, D.W., Lucas, W.J. 1982. Potassium channels in *Chara corallina*. Control and interaction with the electrogenic H^+-pump. *Plant Physiol.* **69:**781–788

Kohler, H.H., Heckmann, K. 1979. Unidirectional fluxes in saturated single-file pores of biological and artificial membranes. I. Pores containing no more than one vacancy. *J. Theor. Biol.* **79:**381–401

Köhler, K., Steigner, W., Simonis, W., Urbach, W. 1985. Potassium channels of *Eremosphaera viridis*. I. Influence of cations and pH on resting potential and an action potential-like signal. *Planta* **166:**490–499

Lühring, H. 1986. Recording of single K^+-channels in the membranes of cytoplasmic drop of *Chara australis*. *Protoplasma* **133:**19–29

Mitchell, P. 1966. Chemiosmotic coupling in oxidative and photosynthetic phosphorylation. *Biol. Rev.* **41:**455–502

Mummert, H., Hansen, U.P., Gradmann, D. 1981. Current-voltage curve of electrogenic Cl^- pump predicts voltage-dependent Cl^- efflux in *Acetabularia*. *J. Membrane Biol.* **62:**139–148

Sanders, D., Hansen, U.P. 1981. Mechanism of Cl^--transport at the plasma membrane of *Chara corallina*: II. Transinhibition and the determination of H^+/Cl^- binding order from a reaction kinetic model. *J. Membrane Biol.* **58:**139–153

Sanders, D., Hansen, U.P., Gradmann, D., Slayman, C.L. 1984. Generalized kinetic analysis of ion-driven cotransport systems: A unified interpretation of selective ionic effects on Michaelis parameters. *J. Membrane Biol.* **77:**123–174

Schroeder, J.I., Hedrich, R., Fernandez, J.M. 1984. Potassium selective single channels in guard cell protoplasts of *Vicia faba*. *Nature* **312:**361–362

Smith, J.R. 1986. Potassium transport across the membranes of *Chara*: II. ^{42}K fluxes and the electrical current as a function of membrane voltage. *J. Exp. Bot.* (*in press*)

Smith, J.R., Smith, F.A., Walker, N.A. 1986. Potassium transport across the membranes of *Chara*: I. The relationships between radioactive tracer influx and electrical conductance. *J. Exp. Bot.* (*in press*)

Sokolik, A.I., Yurin, V.M. 1981. Transport properties of potassium channels of the plasmalemma in *Nitella* cells at rest. *Soviet Plant Physiol.* **28:**206–212

Sokolik, A.I., Yurin, V.M. 1986. Potassium channels in plasmalemma of *Nitella* cells at rest. *J. Membrane Biol.* **89:**9–22

Takeuchi, Y., Kishimoto, U., Ohkawa, T., Kami-Ike, N. 1985. A kinetic analysis of the electrogenic pump of *Chara corallina*: II. Dependence of the pump activity on external pH. *J. Membrane Biol.* **86:**17–26

Tittor, J., Hansen, U.P., Gradmann, D. 1983. Impedance of the electrogenic Cl^- pump in *Acetabularia*: Electrical frequency entrainments, voltage-sensitivity, and reaction kinetic interpretation. *J. Membrane Biol.* **75:**129–139

Tyerman, S.D., Findlay, G.P., Paterson, G.J. 1986*a*. Inward membrane current in *Chara inflata*: I. A voltage- and time-dependent Cl^- component. *J. Membrane Biol.* **89:**139–152

Tyerman, S.D., Findlay, G.P., Paterson, G.J. 1986*b*. Inward membrane current in *Chara inflata*: II. Effects of pH, Cl^-, channel-blockers and NH_4^+, and significance for the hyperpolarized state. *J. Membrane Biol.* **89:**153–161

Received 7 May 1986; revised 19 August 1986